AIP Advances

Ionic conductivity and dielectric permittivity of PEO-$LiClO_4$ solid polymer electrolyte plasticized with propylene carbonate

Cite as: AIP Advances **5**, 027125 (2015); https://doi.org/10.1063/1.4913320
Submitted: 22 November 2014 • Accepted: 09 February 2015 • Published Online: 18 February 2015

S. Das and A. Ghosh

AIP ADVANCES **5**, 027125 (2015)

Ionic conductivity and dielectric permittivity of PEO-$LiClO_4$ solid polymer electrolyte plasticized with propylene carbonate

S. Das and A. Ghosh[a]
Department of Solid State Physics, Indian Association for the Cultivation of Science, Jadavpur, Kolkata 700032, India

(Received 22 November 2014; accepted 9 February 2015; published online 18 February 2015)

We have studied ionic conductivity and dielectric permittivity of PEO-$LiClO_4$ solid polymer electrolyte plasticized with propylene carbonate. Differential scanning calorimetry and X-ray diffraction studies confirm minimum volume fraction of crystalline phase for the polymer electrolyte with 40 wt. % propylene carbonate. The ionic conductivity exhibits a maximum for the same composition. The temperature dependence of the ionic conductivity has been well interpreted using Vogel-Tamman-Fulcher equation. Ion-ion interactions in the polymer electrolytes have been studied using Raman spectra and the concentrations of free ions, ion-pairs and ion-aggregates have been determined. The ionic conductivity increases due to the increase of free ions with the increase of propylene carbonate content. But for higher content of propylene carbonate, the ionic conductivity decreases due to the increase of concentrations of ion-pairs and ion-aggregates. To get further insights into the ion dynamics, the experimental data for the complex dielectric permittivity have been studied using Havriliak–Negami function. The variation of relaxation time with temperature obtained from this formalism follows Vogel-Tamman-Fulcher equation similar to the ionic conductivity. [http://dx.doi.org/10.1063/1.4913320]

I. INTRODUCTION

Recently, major research efforts have been focused on the development of new materials for rechargeable batteries due to depletion of non-renewable resources. Solid polymer electrolytes are the promising electrolyte materials for application in energy storage devices, super capacitors, dye-sensitized solar cells, fuel cells etc.[1–5] Poly (ethylene oxide) (PEO) based solid polymer electrolyte is the most widely investigated system as PEO has low lattice energy and high solvating power for alkali metal salts.[6–10] PEO contains Lewis base ether oxygen which coordinates with the cations and thus help to dissolve the salts.[10] The main drawback of PEO is its low ionic conductivity at room temperature due to the presence of high crystalline phase below the melting temperature.[7] The plasticization is the most common approach to decrease the crystalline phase in polymer and hence to increase the amorphous phase, as it is observed that ion transport becomes enhanced in amorphous phase.[11,12] It has been observed that the addition of low molecular weight organic plasticizer with high dielectric constant such as ethylene carbonate, propylene carbonate, polyethylene glycol, etc. to the polymer matrix decreases the crystalline phase and increases the segmental motion of the polymer chains.[13–16] Incorporation of plasticizer in the polymer matrix may also promote dissociation of ions, thus increasing number of free ions for charge transport. In general, two important parameters such as ionic concentration and ionic mobility influence the conductivity in polymer electrolytes. In this contest the study of ion-ion and ion-polymer interactions is of great interest.[17–19] Electrical conduction

[a]Author for correspondence. E-mail: sspag@iacs.res.in

mechanism in polymer electrolytes arises from the migration of ions coupled with segmental motion of polymer chains.[5] As the segmental motion of polymer chains plays a fundamental role on the transport mechanism,[5] it is necessary to study ion transport mechanism along with polymer segmental relaxation process in polymer electrolytes. The analysis of dielectric spectra is also important to get insights into relaxation phenomena in case of polymers, glasses, oxide ion conductors, etc.[20–22]

In the present work, we have studied ionic conductivity and dielectric relaxation of PEO-$LiClO_4$ solid polymer electrolyte plasticized with propylene carbonate (PC). To illustrate the ion transport mechanism, ion-ion interactions have been also studied using Raman spectra.

II. EXPERIMENTAL PROCEDURE

PEO (M.W 400000, Sigma-Aldrich) and $LiClO_4$ (Sigma-Aldrich) salt were dried in vacuum for preparation of PEO-$LiClO_4$ polymer electrolyte. The molar ratio of ethylene oxide segments to lithium ions was kept at EO/Li=18. Appropriate amounts of PEO and $LiClO_4$ salt were dissolved in acetonitrile and stirred in a magnetic stirrer. The solution became thick after 24 hours due to evaporation of the solvent and was cast in a PTTE container and kept for 24 hours for normal evaporation. At last it was dried for 36 hours at 50°C in vacuum to form free standing homogeneous film. For the preparation of the PEO- $LiClO_4$-X wt. % PC polymer electrolytes, different contents (X = 0, 10, 20, 30, 40 and 50) of PC dispersed in isopropanol were added to solution of PEO and $LiClO_4$ in acetonitrile under stirring condition. The same technique as stated above was followed to get thick films.

X-ray diffraction (XRD) patterns of the prepared films were recorded in an X-ray diffractometer (BRUKER AXS, model D8 ADVANCE) using Cu K_α radiation (0.154 nm wavelength) at a scan rate of 0.3 degree min^{-1}. Differential scanning calorimetry (DSC) experiments (TA instrument, model Q2000) were performed in N_2 atmosphere at a heating scan rate of 10°C min^{-1}. Raman spectra of the samples were recorded at room temperature in a Triple Raman Spectrometer (Jobin-Yvon Horiba, model T64000) attached with a microscope (Olympus, 50 x objectives) using He–Ne laser at 632.817 nm line as the excitation source in the wavelength range of 200 cm^{-1} - 1800 cm^{-1}. Electrical measurements, such as conductance and capacitance of the films were carried out using a RLC meter (Quad Tech, model 7600) in the frequency range 10 Hz – 2 MHz and in a wide temperature range in an anhydrous environment. For the electrical measurements, the films were kept between two stainless steel blocking electrodes of a conductivity cell. Ionic conductivity was determined from the complex impedance plots.

III. RESULTS AND DISCUSSION

XRD patterns of the solid PEO-$LiClO_4$-X wt. % PC electrolytes are shown in Fig. 1. Two strong diffraction peaks at $2\theta = 19°$ and 23.5° are observed due to the semi-crystalline nature of PEO below the melting temperature. It is observed in the figure that the intensity of these diffraction peaks decreases when PC is added to PEO-$LiClO_4$ electrolyte. It is also observed that the peak intensity shows a minimum for 40 wt. % PC. The decrease of the peak intensity indicates that the amorphous phase in the polymer electrolytes increases due to the addition of PC to the polymer electrolytes and it is a maximum for 40 wt. % PC. It is further observed that the intensity of the peaks increases beyond 40 wt. % PC.

DSC traces for different polymer electrolytes, taken during second heating process to remove any thermal history, are shown in Fig. 2. The glass transition temperature (T_g), melting temperature (T_m), and melting enthalpy (ΔH_m) have been calculated from the DSC data and are listed in Table I. It is observed that T_g decreases from 244.79 K to 233.81 K with the addition of PC to PEO-$LiClO_4$ polymer electrolyte. The decreasing value of T_g indicates the increase of the flexibility of polymer backbone which boosts the segmental motion in polymer chains. The crystalline phase has been obtained from the relation $X_C = \Delta H_m/\Delta H_{PEO}$, where ΔH_m is the melting enthalpy of the samples and ΔH_{PEO} is the melting enthalpy (namely 213.7 Jg^{-1}) of completely crystallized PEO.[23] The percentage of crystalline phase of PEO is shown as a function of PC content in the inset of Fig. 2.

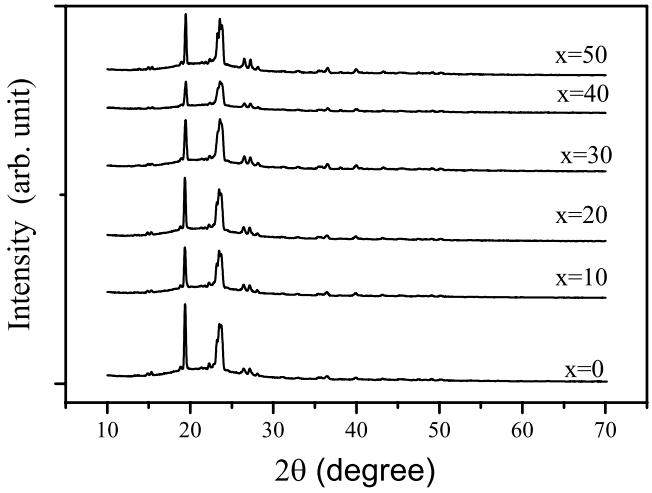

FIG. 1. XRD patterns for different compositions of PEO-$LiClO_4$-X wt. % PC polymer electrolytes.

It is observed that the crystalline phase of PEO decreases up to 40 wt. % PC and hence the volume fraction of the amorphous phase increases with the addition of PC up to 40 wt. %. It is also noted that crystalline phase of PEO increases beyond 40 wt. % PC. These results are consistent with those of XRD.

The reciprocal temperature dependence of the ionic conductivity (σ), obtained from the complex impedance plots, is shown in Fig. 3(a) for different compositions of PEO-$LiClO_4$-x wt. % PC. It is observed that the plots for different compositions in Fig. 3(a) follow Vogel-Tamman-Fulcher (VTF) empirical formula given by[24–26]

$$\sigma = \sigma_0 T^{-1/2} \exp[-E_a/k_B(T-T_0)], \quad (1)$$

where σ_0 is a pre-exponential factor, k_B is the Boltzman constant, E_a is the pseudo activation barrier related to the critical free volume for ion transport, T_0 is the Vogel scaling temperature where the

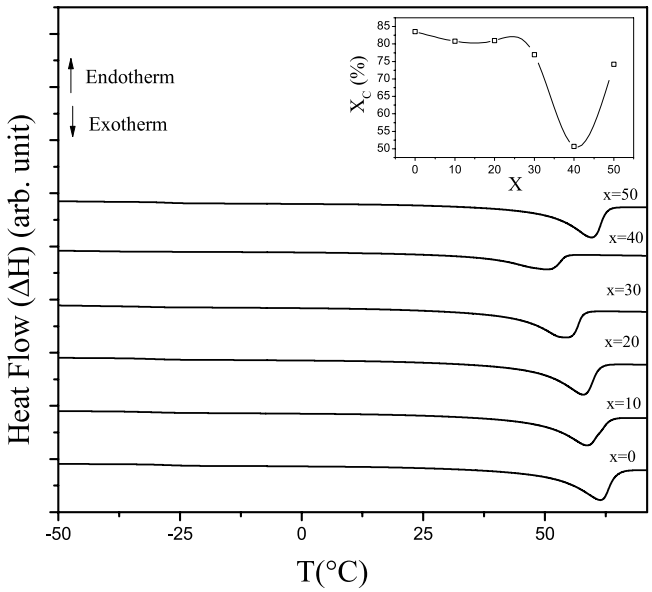

FIG. 2. DSC thermo-grams for different compositions of PEO-$LiClO_4$-X wt. % PC electrolytes. Inset shows the variation of percentage of crystalline phase X_C (%) with PC content.

TABLE I. Glass transition and melting temperatures, percentage of crystalline phase (X_C %), E_a and T_0 obtained from VTF formalism for PEO-$LiClO_4$-X wt. % PC electrolytes.

PC content X (wt. %)	T_g (K) (±0.02)	T_m (K) (±0.02)	X_C (%)	E_a (eV) (±0.002)	T_0 (K) (±2)
0	244.79	334.38	39.08	0.094	174
10	243.96	331.63	37.81	0.107	164
20	242.73	330.84	37.90	0.146	154
30	242.21	326.98	36.01	0.073	171
40	233.81	323.27	23.70	0.092	157
50	245.84	332.48	34.70	0.112	167

configurational entropy or the critical volume becomes zero and T is the absolute temperature. The conductivity data presented in Fig. 3(a) have been fitted to Eq. (1) by the best fit method. Good fits to VTF formula in the entire temperature range clearly indicate that the Li^+ ionic motion is coupled with the polymer segmental motion in these polymer electrolytes. The parameters obtained from VTF fits are shown in Table I. It is observed in the table that the values of (T_g–T_0) are in the range 70 K - 80 K, which is consistent with the values observed for other PEO bases electrolytes. We have also shown the composition dependence of the ionic conductivity in Fig. 3(b). It is noted that at low content of PC the conductivity does not increase significantly, but above 20 wt. % PC the conductivity increases rapidly with the increase of PC content and shows a maximum at 40 wt.

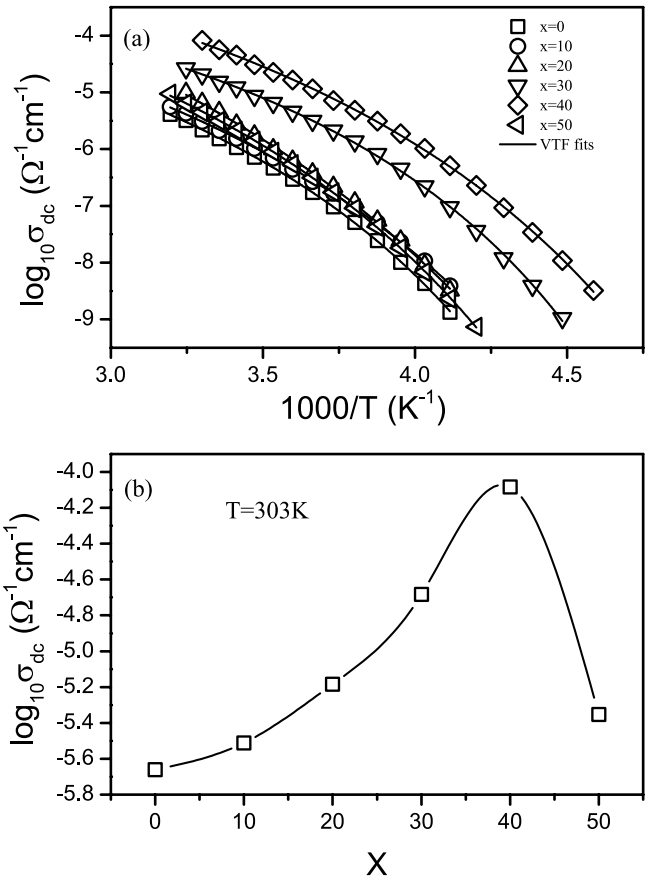

FIG. 3. (a) Reciprocal temperature dependence of the ionic conductivity for different compositions PEO-$LiClO_4$-X wt. % PC electrolytes. Solid lines are fits to VTF. (b) Variation of the ionic conductivity at 303K with PC content.

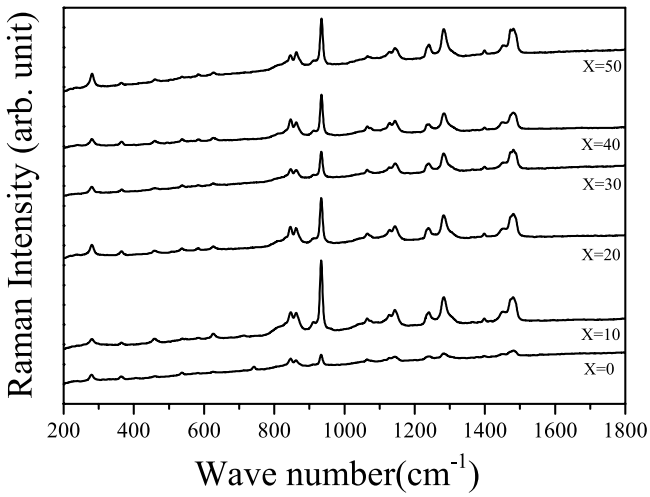

FIG. 4. Raman spectra for different compositions of PEO-$LiClO_4$-X wt. % PC in the wave number range of 200 cm^{-1} - 1800 cm^{-1}.

% PC. The addition of PC in polymer increases interactions between different ion species such as ClO_4^- anions, Li^+ cations, carbonyl oxygen in PEO and lone pair electron of the C=O bond of PC. The interaction between PC and Li^+ (basically the lone pair electron of C=O bond and other oxygen atom in the ring structure of PC) increases the flexibility of the PEO matrix and thus Li^+ ions conduct with high mobility. With the addition of PC, there is an interaction between PEO and PC via Li^+ ions, since the PC-Li^+ ion interaction is not stronger than PEO-Li^+ ion interaction.[16] At low content of PC, formation of PC - Li^+ is less so that the conductivity does not increase considerably. But with the increasing PC content there is a new path (PEO-Li^+ -PC) for Li^+ ion conduction, which increases the conductivity rapidly.[16] With higher content (50 wt. %) of PC, the ionic conductivity decreases due to increase in ion-pairs concentration as obtained from the analysis of the Raman spectra below.

Raman spectra of all samples in the wave number range 200 cm^{-1} to 1800 cm^{-1} are shown in Fig. 4. The different peaks observed in the spectra correspond to ion-ion and ion-polymer interactions in the polymer electrolytes. We have correlated ionic conductivity with ion-ion interactions. We have analyzed Raman peak observed in the range 910 cm^{-1} to 950 cm^{-1}, which is associated with free ions, ion pairs and ion aggregates. The de-convolution of the peak, using Gaussian-Lorentzian product function, is shown in Fig. 5 for a composition. Fig. 5(a) indicates that this single peak consists of three peaks at 933 cm^{-1}, 925 cm^{-1} and 937 cm^{-1} which correspond to the modes of the free ions, ion-aggregates and ion-pairs respectively.[17,18] The relative integrated intensity of the peak at 933 cm^{-1} for free ions is shown in Fig. 5(b) as a function of PC content. The variation of the relative intensity of ion- pairs and ion- aggregates with PC content is also shown in the inset of Fig. 5(b). It is observed that the relative intensity of the free ions, which is proportional to the relative concentration of free ions, shows an increasing trend with the increase of PC content, which in turn indicates an increase in the conductivity with the increase of PC content in the polymer electrolytes. The maximum conductivity is observed for 40 wt. % PC due to maximum intensity of the free ions for this composition. The addition of PC beyond 40 wt. % increases concentration of ion-pairs and ion-aggregates and as a result the concentration of free ions decreases and thus the conductivity decreases.

The frequency dependence of the real $\varepsilon'(\omega)$ and imaginary $\varepsilon''(\omega)$ parts of the dielectric permittivity $\varepsilon^*(\omega)$, known as dielectric constant and dielectric loss respectively, is shown in Figs. 6(a) and 6(b) respectively at several temperatures. The variation of $\varepsilon'(\omega)$ at 293 K with PC content is shown in the inset of Fig. 6(a). It is observed in Fig. 6(a) that the value of $\varepsilon'(\omega)$ decreases with the increase in frequency and shows a labelling-off as usual at higher frequencies denoted by ε_∞, which

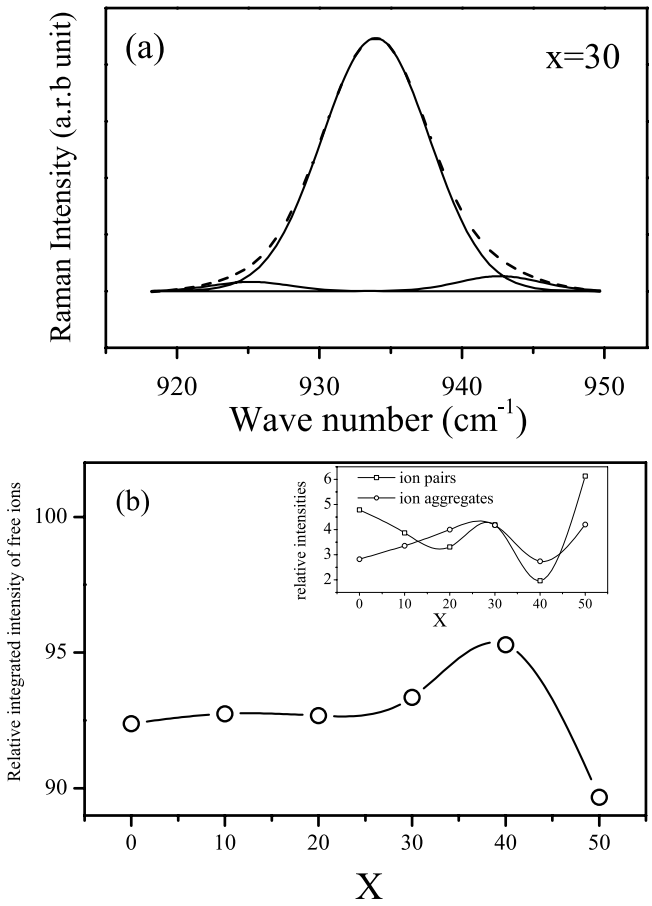

FIG. 5. (a) De-convoluted Raman spectra in the region 900 cm^{-1} to 980 cm^{-1} of PEO-$LiCLO_4$-30 wt. % PC. The experimental data are shown by dashed lines and the de-convoluted lines are shown by solid lines. (b) Variation of relative integrated intensity of free ions with PC content for PEO-$LiCLO_4$-X wt. % PC electrolytes. The variation of relative integrated intensity of ion-pairs and ion-aggregates with PC content is shown in the inset.

originates mainly from the rapid polarization of atoms and electrons due to the application of a time dependent electric field. It is noticed that with the addition of PC, the value of $\varepsilon'(\omega)$ increases up to 40 wt. % PC, but the increase is not significant in the high frequency region. Incorporation of PC in the polymer matrix may increase localization of charge carriers including mobile Li^+ ions which is possibly responsible for higher $\varepsilon'(\omega)$ value of PEO-$LiClO_4$-PC polymer electrolytes than that of PEO-$LiClO_4$ polymer electrolyte. The value of $\varepsilon'(\omega)$ also increases with the increase in temperature as shown in Fig. 6(a). The strong increase of $\varepsilon'(\omega)$ at lower frequencies is due to the contribution of interface and electrode polarization to the impedance of the samples. It is noticed in Fig. 6(b) that in the low frequency side the value of $\varepsilon''(\omega)$ increases as the long range hopping of mobile ions is accounted for polarization and as the frequency decreases, the value of $\varepsilon''(\omega)$ increases rapidly. The experimental data for $\varepsilon'(\omega)$ and $\varepsilon''(\omega)$ have been analyzed using Havriliak–Negami (HN) formalism,[27–29] in which the complex dielectric function is given by

$$\varepsilon^*(\omega) = \varepsilon_\infty + \left[\frac{\varepsilon_s - \varepsilon_\infty}{[1 + (i\omega\tau_{HN})^{\alpha_{HN}}]^{\gamma_{HN}}}\right], \tag{2}$$

where ε_s and ε_∞ are the static and high frequency dielectric constants respectively, τ_{HN} is the relaxation time. α_{HN} and γ_{HN} are the shape parameters with values $0 \le \alpha_{HN} < 1$ and $0 \le \alpha_{HN}\gamma_{HN} < 1$. When the values of α_{HN} and γ_{HN} are unity, Debye relaxation is obtained and the non-zero value corresponds to

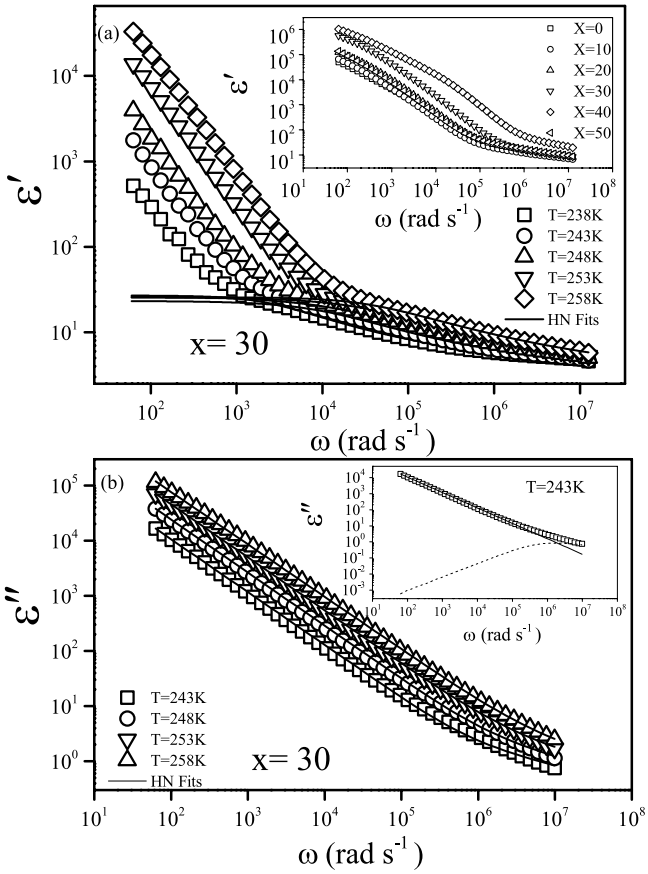

FIG. 6. Frequency dependence of (a) dielectric constant $\varepsilon'(\omega)$ and (b) dielectric loss $\varepsilon''(\omega)$ at several temperatures for PEO-$LiClO_4$-30 wt. % PC respectively. Inset in (a) shows frequency dependence of $\varepsilon'(\omega)$ for different compositions. The contributions of the conductivity and dielectric relaxation at a fixed temperature are shown by solid and dotted lines respectively in the inset of (b).

a distribution of relaxation times. In presence of electrode polarization, the static dielectric constants ε_s is determined in the plateau-like region near the intermediate frequency range shown in Fig. 6(a).

The real and imaginary parts of $\varepsilon^*(\omega)$ are respectively expressed as

$$\varepsilon'(\omega) = \varepsilon_\infty + (\varepsilon_s - \varepsilon_\infty)\left[1 + 2(\omega\tau_{HN})^{\alpha_{HN}}\cos(\alpha_{HN}\pi/2) + (\omega\tau_{HN})^{2\alpha_{HN}}\right]^{-\gamma_{HN}/2}$$
$$\times\cos\left[\arctan\left[\frac{\sin(\alpha_{HN}\pi/2)}{[(\omega\tau_{HN})^{-\alpha_{HN}} + \cos(\beta_{HN}\pi/2)]}\right]\right] \quad (3)$$

TABLE II. Dielectric strength (ε_s-ε_∞), shape parameters α_{HN} and γ_{HN}, exponent n, E_a and T_0 obtained from VTF fits for relaxation time for PEO-$LiClO_4$-X wt. % PC electrolytes.

PC content X (wt. %)	$\Delta\varepsilon = \varepsilon_s$-$\varepsilon_\infty$ (±1) T=253K	α_{HN} (±0.02) T=253K	γ_{HN} (±0.02) T=253K	n (±0.05) T=253K	E_a (eV) (±0.002)	T_0 (K) (±2)
0	19	0.86	0.52	0.91	0.040	192
10	16	0.73	0.71	0.92	0.046	199
20	28	0.78	0.57	0.92	0.022	208
30	20	0.76	0.54	0.94	0.016	211
40	53	0.70	0.56	0.94	0.037	182
50	19	0.84	0.51	0.94	0.005	210

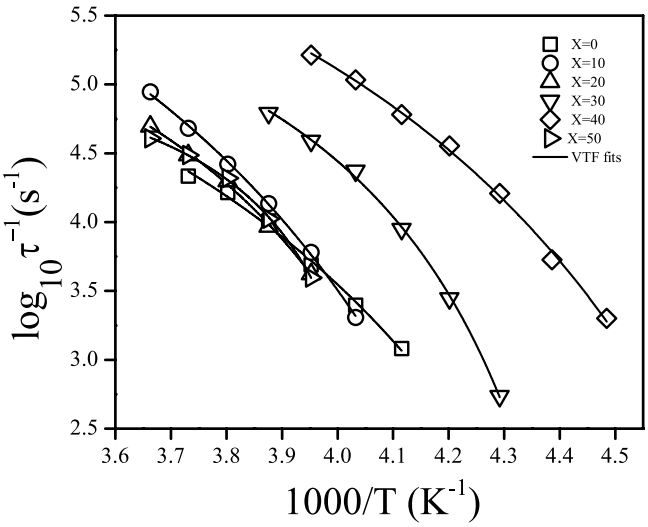

FIG. 7. Reciprocal temperature dependence of the inverse relaxation time τ_{HN} for different compositions of PEO-$LiCLO_4$-X wt. % PC electrolytes. Solid lines are fits to VTF equation.

and

$$\varepsilon''(\omega) = (\varepsilon_s - \varepsilon_\infty)\left[1 + 2(\omega\tau_{HN})^{\alpha_{HN}}\cos(\alpha_{HN}\pi/2) + (\omega\tau_{HN})^{2\alpha_{HN}}\right]^{-\gamma_{HN}/2}$$
$$\times \sin\left[\arctan\left[\frac{\sin(\alpha_{HN}\pi/2)}{[(\omega\tau_{HN})^{-\alpha_{HN}} + \cos(\alpha_{HN}\pi/2)]}\right]\right] + \frac{S}{\omega^n} \quad (4)$$

The extra term $\frac{S}{\omega^n}$ is added to Eq. (4) to account for the contribution of electrode polarization. The value of n is in the range $0 < n < 1$ and the unit value of n signifies ideal Ohmic behaviour. The experimental data for $\varepsilon'(\omega)$ and $\varepsilon''(\omega)$, presented in Figs. 6(a) and 6(b), have been fitted simultaneously to Eqs. (3) and (4) respectively. The values of $\Delta\varepsilon = \varepsilon_s$-$\varepsilon_\infty$, shape parameters ($\alpha_{HN}$ and γ_{HN}) and exponent n obtained from the best fits are shown in Table II for different compositions. The value of n is less than unity, indicating a deviation from Ohmic behaviour in the polymer electrolytes. In the inset of Fig. 6(b) the contribution of the ionic conductivity is shown by solid lines, while that of relaxation are shown by dotted lines. It is also observed that no distinct peak is observed as the ionic conductivity suppresses the relaxation peak. Similar behaviour has been also observed for other compositions. Fig. 7 shows the plots of the inverse of dielectric relaxation time τ_{HN} against reciprocal temperature. It is observed that the relaxation time τ_{HN} is fitted well to the VTF equation. The obtained parameters for the best fits are listed in Table II. It should be noted that the relaxation time decreases and relatively fast segmental motion coupled with mobile ions enhances the transport properties in the polymer electrolytes with the addition of PC.

IV. CONCLUSIONS

The addition of plasticizer PC in the PEO-$LiClO_4$ polymer electrolyte decreases the crystallinity in the PEO polymer matrix. The content of free ions increases up to 40 wt. % of PC increasing the ionic conductivity, while for the high content of PC beyond 40 wt. %, the contribution of ion-pairs and ion-aggregates dominates leading to a decrease in the conductivity. The dielectric constants increase with the addition of PC in the polymer electrolyte. The shape parameters α_{HN} and γ_{HN} for dielectric relaxation are almost composition independent. The reciprocal temperature dependence of the ionic conductivity and the relaxation time shows VTF nature, and the parameters obtained from the fits of the experimental data to the VTF equation indicate a wide distribution of relaxation times.

[1] *Applications of Electroactive Polymers*, edited by B. Scrosati (Chapman and Hall, London, 1993).
[2] *Solid Polymer Electrolytes–Fundamentals and Technological Applications*, edited by F.M. Gray (VCH, New York, 1991).

[3] G. Mao, R.F. Perea, and W.S. Howells, Nature **405**, 163 (2000).
[4] J.Y. Song, Y.Y. Wang, and C.C. Wan, J. Power Sources **77**, 183 (1999).
[5] B.W.H. Meyer, Adv. Mater. **10**, 439 (1998).
[6] G. B. Appettecchi, P. Romagnoli, and B. scrosati, Electrochem. Commun. **3**, 281 (2001).
[7] T. Itoh, Y. Miyamura, Y. Ichikawa, T. Uno, M. Kubo, and O. Yamamoto, J. Power Sources **119-121**, 403 (2003).
[8] I. Nicotera, G. Antonio, M. Terenzi, A.V Chadwick, and M.I. Webster, Solid State Ionics **146**, 143 (2002).
[9] A. Karmakar and A. Ghosh, Curr. Appl. Phys. **12**, 539 (2012).
[10] P. Lightfoot, M.A. Mehta, and P.G. Bruce, Science **262**, 883 (1993).
[11] Y. Kim and E.S. Smotkin, Solid State Ionics **149**, 29 (2002).
[12] M. Forsyth, D.R. Macfarlane, A. Best, J. Adebahr, P. Jacobsson, and A.J. Hill, Solid State Ionics **147**, 203 (2002).
[13] Y. Li, J. Wang, J. Tang, Y. Liu, and Y. He, J. Power Sources **187**, 305 (2009).
[14] Y. Masuda, M. Seki, M. Nakayama, M. Wakiharav, and H. Mita, Solid State Ionics **177**, 843 (2006).
[15] H.J. Woo, S.R. Majid, and A. K. Arof, Solid State Ionics **252**, 102 (2013).
[16] R.J. Sengwa and S. Choudhary, Indian J. Phys. **88**, 461 (2014).
[17] S. Schantz, J. Chem. Phys. **94**, 6296 (1991).
[18] S. Schantz, L.M. Torell, and J.R. Stevens, J. Chem. Phys. **94**, 6862 (1991).
[19] M. Deepa, S. Agnihotry, D. Gupta, and R. Chandra, Electrochim. Acta **49**, 373 (2004).
[20] S.K. Chaurasia, R.K. Singh, and S. Chandra, J. Polym. Sci. Part B Polym. Phys. **49**, 291 (2011).
[21] B. Deb and A. Ghosh, J. Appl. Phys. **108**, 074104 (2010).
[22] T. Paul and A. Ghosh, J. Appl. Phys. **116**, 144102 (2014).
[23] X. Li and S. L. Hsu, and J. Polym. Sci., Polym. Phys. Ed. **22**, 1331 (1984).
[24] H. Vogel, Z. Phys. **22**, 645 (1921).
[25] G. Tamman and W. Hesse, Z. Anorg. Allg. Chem. **156**, 245 (1926).
[26] G. S. Fulcher, J. Am. Ceram. Soc. **8**, 339 (1925).
[27] S. Havriliak and S. Negami, Polymer **8** (1967).
[28] C. Iacob, J.R. Sangoro, a Serghei, S. Naumov, Y. Korth, J. Kärger, C. Friedrich, and F. Kremer, J. Chem. Phys. **129**, 234511 (2008).
[29] S. Cobo, T. Mahfoud, E.J.M. Vertelman, P.J. Van Koningsbruggen, P. Demont, and A. Bousseksou, J. Phys. Chem. C **113**, 2586 (2009).